آنالیز حالت گذرا و حالت ماندگار لیزرهای کوانتومی آبشاری با استفاده از الگوی مدار معادل

حسین رضا یوسف وند[1]

[1]دانشکده مهندسی برق و کامپیوتر، دانشگاه آزاد اسلامی واحد اسلامشهر، تهران.

چکیده – در این مقاله یک الگوی مداری جدید به منظور شبیه سازی مشخصه های حرارتی در لیزرهای کوانتومی آبشاری *(QCLs)* ارائه شده است. این مدار معادل با بکارگیری برخی از الگوهای کوانتومی استاندارد از قبیل معادله ترابری همدوس، معادلات آهنگ چهار سطحی ساده شده و معادله انتقال حرارت گسترش یافته است. به منظور مدلسازی رفتار افزاره، مدار معادل ارائه شده به سه مدار تعاملی مجزا تجزیه می شود: ۱) یک مدار بایاس برای توصیف ترابری همدوس و استخراج مشخصه جریان-ولتاژ در افزاره، ۲) یک مدار اصلی، شامل معادلات آهنگ و توصیف کننده دینامیک حامل در ناحیه فعال لیزر، ۳) یک مدار حرارتی، برای احتساب تلفات حرارتی در افزاره. با استفاده از الگوی ارائه شده مشخصه های حرارتی یک لیزر کوانتومی آبشاری در شرایط ایستا و پویا مورد بررسی قرار می گیرد. مقایسه نتایج حاصل از الگوی ارائه شده و نتایج تجربی منتشر شده از تطابق بسیار خوبی برخوردار می باشند و این مقایسه ارزش الگوی ارائه شده را تایید می نماید.

کلید واژه– لیزر کوانتومی آبشاری، مشخصه های حرارتی، مدار معادل.

Transient and Steady State Analysis of Quantum Cascade Lasers Using Equivalent Circuit Model

Hossein Reza Yousefvand[1]

[1] Department of Electrical and Computer Engineering, Islamshahr Branch, Islamic Azad University, Tehran, Iran.

Abstract- In this paper, to simulate the temperature-dependent output characteristics of quantum cascade lasers (QCLs) we present a new circuit-level model. The equivalent circuit model of the laser by employing a number of standard quantum mechanical approaches such as the carrier coherent transport, a simplified four-level carrier scattering rates and heat transfer equation is developed. The presented equivalent circuit can be divided in three interactive circuits including: the biasing circuit that accounts for the coherent transport using sequential resonant tunneling to adopt the current-voltage relationship in the device; the intrinsic QCL circuit that includes the rate equations describing the carrier dynamics inside the device active region levels; the thermal circuit, which incorporates the heat dissipation. Using the presented model, the thermal characteristics of a QCL under the steady and dynamic conditions are investigated. The excellent agreement of the experimental data with the simulated temperature-dependent light output-current characteristics confirms the validity of the model.

Keywords: Quantum cascade laser, Thermal effects, Equivalent circuit.

Transient and Steady State Analysis of Quantum Cascade Lasers Using Equivalent Circuit Model

Hossein Reza Yousefvand
hossein@iiau.ac.ir

1 Introduction

Quantum cascade lasers (QCLs) are semiconductor injection lasers based on optical and electronic intersubband transitions (ISTs) between quantized intersubband levels in multiple quantum structures [1]. Compared with conventional semiconductor lasers, QCLs suffer from two distinct effects [2]: 1) the Stark-effect rollover, i.e., is due to an increase in voltage across the device which causes a misalignment between the ground state of injector and the upper energy levels in the active region, and 2) the large threshold current which lead to strong local heating effects inside the device active regions. In this paper, we extended the theoretical model of our previous works [3], [4] and developed a comprehensive circuit-level implementation of QCLs to analyze the temperature and bias dependent characteristics of the device.

2 Physics and Theory

A schematic representation of the dynamical processes occurring within a QCL active-region is given in Fig.1. As shown in the figure, electrons are injected from injector ground-state g into upper laser state 3. The injected carriers into state 3 scatter radiatively into the lower laser state 2, or follow other nonradiative scattering paths. Thermal backfilling current into the state 2 from the next injector ground state g′, as well as the thermionic emission from the states 4 and 5 into the continuum states, are also included in the model.

2.1 Carrier Coherent Transport

In the QC laser, carrier injection is accomplished by the resonant tunneling (RT) of electrons from the injector ground state g into the excited state 3,

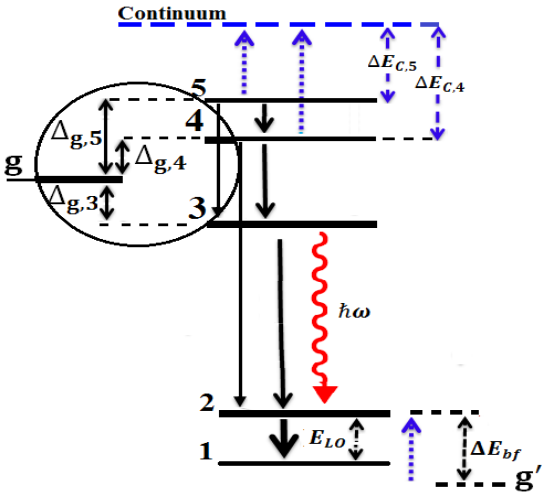

Figure 1: Schematic representation of a 5-level QCL-active region with the various relaxation processes indicated by arrows.

and carriers are transferred until these states are alignment. As the bias is increased furthermore, the injector ground state is brought in resonance with the other states 4 and 5, sequentially, which creates the leakage current path for the device in parallel with the injection into the state 3 [5]. Based on this concept, we can then easily find the device current I_{Inj} by summing over the contributions from each tunnelling transition component, $I_{inj} = I_{g,3} + I_{g,4} + I_{g,5}$.

Based on density matrix approach, the current between injector ground state g and upper state i (=3, 4, 5) is expressed as [5]

$$I_{g,i} = qAN_S \frac{2\left|\Omega_{g,i}\right|^2 \tau_\perp}{1 + \Delta_{g,i}^2 \tau_\perp^2 + 4\left|\Omega_{g,i}\right|^2 \tau_i \tau_\perp} \qquad (1)$$

where q is the electronic charge, N_S is the sheet density in the injector, A is the device area, $\hbar\Delta_{g,i}$ is the energy detuning between injector ground state g and state i, which obtained as a function of applied electric field [4]. $\hbar\Omega_{g,i}$ (= 2 meV) is the coupling energy between the injector ground state

g and the state i. τ_i is the temperature-dependent LO phonon scattering lifetime of an electron in the state i and $\tau_\perp$ is the relaxation time for the momentum in the plane of the layer, responsible for the loss of phase between the states involved in RT, an estimate for $\tau_\perp$ in the 10-300 K range is 100-50 fs [5]. Finally, we assume a linear relation between the device voltage V and the total device current I_{Inj} above the laser threshold, as [6]

$$V = V_{th} + (I_{Inj} - I_{th})R_d \tag{2}$$

where V_{th} and R_d respectively denote the threshold voltage and differential resistance, and already been introduced in [7]. I_{th} denotes the temperature-dependent device threshold current including the three components: 1) the intrinsic threshold current I_{th0} to overcome the waveguide and mirror losses [8], 2) the leakage current I_{esc} due to escape of electrons from the upper states 4 and 5 into continuum [4], and 3) the backfilling current I_{bf} due to thermal backfilling of electrons from the downstream electron reservoir into the lower lasing state of the previous stage [9]. In that case, the total laser threshold current can be written as

$$I_{th} = I_{th0} + I_{esc} + I_{bf} \tag{3}$$

2.2 Carrier and Photon Dynamics

The system of rate equations relating the electron numbers N_5, N_4, N_3 and N_2, the photon number N_P and their time derivatives, taking into account the sequential resonant tunnelling concept, can be expressed as previous work [4]

$$\frac{dN_5}{dt} = \frac{I_{g,5}}{q} - \frac{N_5}{\tau_5} - \frac{N_5}{\tau_{th,5}} \tag{4}$$

$$\frac{dN_4}{dt} = \frac{I_{g,4}}{q} + \frac{N_5}{\tau_{54}} - \frac{N_4}{\tau_4} - \frac{N_4}{\tau_{th,4}} \tag{5}$$

$$\frac{dN_3}{dt} = \frac{I_{g,3}}{q} - \frac{N_3}{\tau_3} + \frac{N_5}{\tau_{53}} + \frac{N_4}{\tau_{43}} - \Gamma\frac{c'\sigma_{32}}{V_m}(N_3 - N_2)N_P \tag{6}$$

$$\frac{dN_2}{dt} = \frac{N_3}{\tau_{32}} + \frac{N_4}{\tau_{42}} - \frac{N_2}{\tau_2} + \Gamma\frac{c'\sigma_{32}}{V_m}(N_3 - N_2)N_P + \frac{I_{bf}}{q} \tag{7}$$

$$\frac{dN_P}{dt} = -\frac{N_P}{\tau_P} + N\Gamma\frac{c'\sigma_{32}}{V_m}(N_3 - N_2)N_P + N\beta\frac{N_3}{\tau_{SP}} \tag{8}$$

All of the parameters have been introduced in the previous work [4].

2.3 Self-Heating Effect

To incorporate the self-heating effect in the model, we use VCSEL-like thermal rate equation that accounts for the transient temperature increases of core temperature as a result of heat sink temperature [10], [11]. Following this approach we can write

$$T = T_S + \sigma(I_{Inj}V - P_o)R_{TH} - \tau_T\frac{dT}{dt} \tag{10}$$

where T_S is the sink temperature, V is the device voltage defined by equation (2), P_o is the output optical power, R_{TH} is the QCL's thermal resistance, σ denotes the duty cycle in pulse operation, τ_T is the thermal time constant (which represents heat initially escaping from the active region into the waveguide cladding and insolation layers primarily.

3 Circuit-Level Implementation

The HSPICE implementation depends on transformation of physically based equations into the equivalent circuit representation. Based on this concept, we obtain a complete circuit model to simulate the behaviour of device in both the steady and dynamic conditions. As illustrated in Fig. 2, the total equivalent circuit describing the QCL's behaviour is composed of three interactive circuits: the input circuit to model the voltage-current relationship defined in (2), the intrinsic QCL-circuit to model the carrier dynamics inside the various levels, and thermal circuit to model the self-heating effect. In order to extract the intrinsic QCL-circuit, proportional to carrier and photon numbers in rate equations of (4)-(8), we define new circuit-variable of V_i (i = 2, 3, 4, 5) and V_P scaled with the arbitrary constants z_n and k, and to obtain better convergence the square of V_P is used [3]

$$N_i = z_n \cdot V_i\Big|_{z_n \approx 10^{15}} \tag{11}$$

$$N_P = \frac{(V_P + \delta)^2}{k}\Big|_{k \approx 1.5\cdot 10^{-19}} \qquad \delta \geq 0 \tag{12}$$

where N_i, and N_P denote the carrier and photon numbers, respectively. Therefore, the quantities N_2, N_3, N_4, N_5 and N_P in (4)-(8) scaled to circuit variables V_2, V_3, V_4, V_5 and V_P, respectively.

4 Results and Discussion

In the simulation, the laser is a standard InP-based lattice matched $In_{0.52}Al_{0.48}As/In_{0.53}Ga_{0.47}As$ QCL designed for Mid- IR wavelengths [12]. The calculated electric field-current and light-current characteristics of the device for different values of sink temperature are illustrated in Figs. 3(a) and 3(b), respectively. It can be seen that the current components $I_{g,3}$, $I_{g,4}$ and $I_{g,5}$, which are qualitatively similar in behaviour, are sensitive to the electric field. Additionally, in Fig. 3(b), in order to validate the predicted values of our model,

we compare the simulated L-I characteristics with experimental data reported in [12], under the different values of

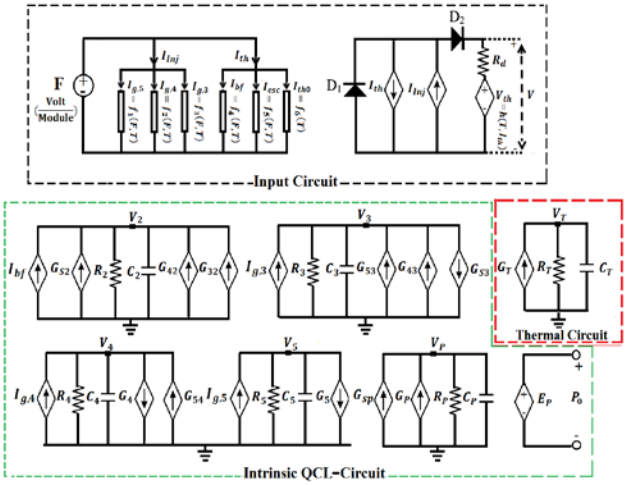

Figure 2: Circuit-level implementation of Mid-IR QCLs.

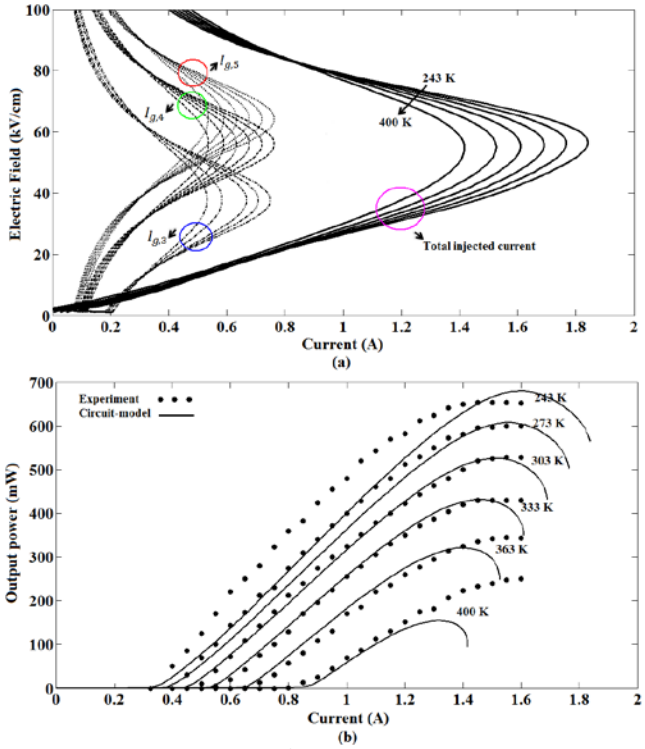

Figure 3: Simulated (a) electric field and (b) light output powers as a function of total injected current, for a range of sink temperatures.

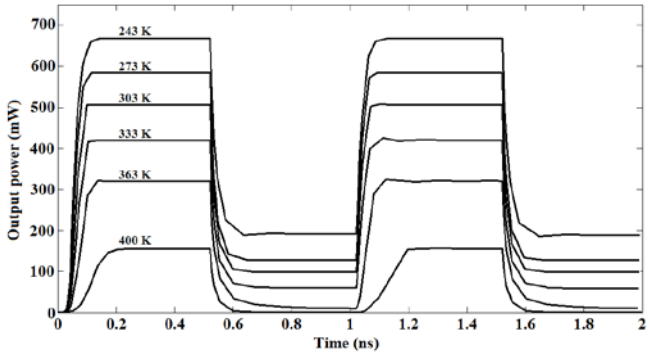

Figure 4: Transient response of the laser output power at the various sink temperatures under a pulse electric field.

Sink temperature. The results show acceptable agreement between threshold current, slope efficiency and output power degradation for simulated and experimental data. The temporal evolution of light output power under an applied electric field (1 ns pulse) varying between 15 and 40 kV/cm with 1 ps rise and fall times, at different sink temperatures is illustrated in Fig. 4. As we can see, by increasing the sink temperature, output power is degraded.

5 Conclusion

By employing a number of optoelectronic approaches, a comprehensive circuit-level model that account for the thermal and field dependence of a QCL's behaviour has been developed. Using the presented model, the steady and dynamic performances of the device were investigated All simulation results indicate that the presented circuit model can be a very useful tool for analyzing and optimizing QCL designs.

References

[1] J. Faist, F. Capasso, D. L. Sivco, C. Sirtori, A. L. Hutchinson, and A. Y. Cho, "Quantum cascade laser," *Science*, vol. 264, pp. 553-556, 1994.

[2] S. S. Howard, Z. J. Liu, and C. F. Gmachl, "Thermal and Stark-Effect roll-Over of quantum-cascade lasers," *IEEE J. Quantum Electron.*, vol. 44, no. 4, pp. 319-323, 2008.

[3] H. R. Yousefvand, V .Ahmadi, and K .Saghafi, "Static and dynamic response analysis of Raman injection quantum cascade laser using circuit level modeling," *J. Lightwave Technol.*, vol. 28, no. 21, pp. 3142-3148, 2010.

[4] H. R. Yousefvand, and V. Ahmadi, "Optical and transport characteristics of Raman injection laser with enhanced Stokes emission," *J. Opt. Soc. Am. B*, vol. 32, no. 5, pp. 861-867, 2015.

[5] C. Sirtori, F. Capasso, J. Faist, A. L. Hutchinson, D. L. Sivco, and A. Y. Cho, "Resonant tunneling in quantum cascade lasers," *IEEE J. Quantum Electron.*, vol. 34, pp. 1722–1729, 1998.

[6] M. Razeghi, "High-performance InP-Based Mid-IR quantum cascade lasers," *IEEE J. Sel. Topics. Quantum Electron.*, vol. 15, no. 3, pp. 941-951, 2009.

[7] C. Gmachl, F. Capasso, A. Tredicucci, D. L. Sivco, R. Kohler, A. L. Hutchinson, and A. Y. Cho, "Dependence of the device performance on the number of stages in quantum-cascade lasers," *IEEE J. Sel. Topics. Quantum Electron.*, vol. 5, no. 3, pp. 808-816, 1999.

[8] S. S. Howard, Z. J. Liu, D. Wasserman, A. J. Hoffman, T. S. Ko, and C. F. Gmachl, "High-performance quantum cascade lasers: optimized design through waveguide and thermal modeling," *IEEE J. Sel. Topics Quantum Electron.*, vol. 13, no. 5, pp. 1054-1064, 2007.

[9] Z. M. Simon Li, Y. Y. Li, and G. P. Ru, "Simulation of quantum cascade lasers," *J. Appl. Phys.*, vol. 110, pp. 093109-1-093109-7, 2011.

[10] P. V. Mena, J. J. Morikuni, S.-M. Kang, A.V. Harton, and K. W. Wyatt, "A simple rate-equation-based thermal VCSEL model," *J. Lightwave Technol.*, vol. 17, no. 5, pp. 865-872, 1999.

[11] G. Monastyrskyi, M. Elagin, M. Klinkmuller, A. Aleksandrova, S. Kurlov, Y. V. Flores, J. Kischkat, M. P. Semtsiv, and W. T. Masselink, " Impact of heat dissipation on quantum cascade laser performance," *J. Appl. Phys.*, vol. 113, pp. 134509-1-134509-6, 2013.

[12] A. Wittmann, Y. Bonetti, J. Faist, E. Gini, and M. Giovannini, “Intersubband linewidth in quantum cascade laser designs,” *Appl. Phys. Lett.*, vol. 93, pp. 141103-1-141103-3, 2008.